Metallomics

Accepted Manuscript

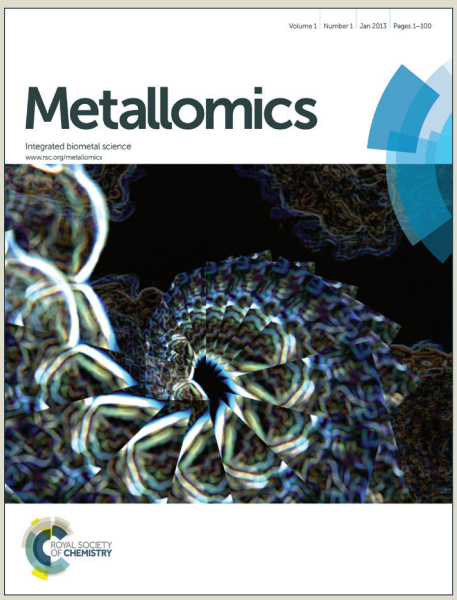

ROYAL SOCIETY OF CHEMISTRY

www.rsc.org/metallomics

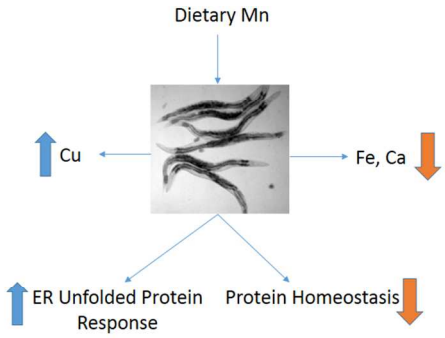

Mn feeding induces altered metal composition and degrades protein homeostasis in C. elegans
338x190mm (96 x 96 DPI)

Journal Name

RSCPublishing

ARTICLE

Manganese Disturbs Metal and Protein Homeostasis in *Caenorhabditis elegans*

Cite this: DOI: 10.1039/xoxxoooooox

Received ooth January 2012,
Accepted ooth January 2012

DOI: 10.1039/xoxxoooooox

www.rsc.org/

Suzanne Angeli[a], Tracy Barhydt[a], Ross Jacobs[a], David W. Killilea[b], Gordon J. Lithgow[a] and Julie K. Andersen[a]

Parkinson's disease (PD) is a debilitating motor and cognitive neurodegenerative disorder for which there is no cure. While aging is the major risk factor for developing PD, clear environmental risks have also been identified. Environmental exposure to the metal manganese (Mn) is a prominent risk factor for developing PD and occupational exposure to high levels of Mn can cause a syndrome known as manganism, which has symptoms that closely resemble PD. In this study, we developed a model of manganism in the environmentally tractable nematode, *Caenorhabditis elegans*. We find that, in addition to previously described modes of Mn toxicity, which primarily include mitochondrial dysfunction and oxidative stress, Mn exposure also significantly antagonizes protein homeostasis, another key pathological feature associated with PD and many age-related neurodegenerative diseases. Mn treatment activates the ER unfolded protein response, severely exacerbates toxicity in a disease model of protein misfolding, and alters aggregate solubility. Further, aged animals, which have previously been shown to exhibit decreased protein homeostasis, are particularly susceptible to Mn toxicity when compared to young animals, indicating the aging process sensitizes animals to metal toxicity. Mn exposure also significantly alters iron (Fe) and calcium (Ca) homeostasis, which are important for mitochondrial and ER health and which may further compound toxicity. These finding indicate that modeling manganism in *C. elegans* can provide a useful platform for identifying therapeutic interventions for ER stress, proteotoxicity, and age-dependent susceptibilities, key pathological features of PD and other related neurodegenerative diseases.

Introduction

Parkinson's disease (PD) is a multifactorial disease in which aging, genetic susceptibility, and environmental insults all contribute to its onset. It is characterized by dopaminergic degeneration, which leads to a host of characteristic motor dysfunctions, including tremor, rigidity, and bradykinesia. Environmental exposure to metals, especially manganese, is an established risk factor for the development of PD[1]. Manganese (Mn) can be found in water purifiers, drinking water, fungicides, gasoline additives, and airborne pollutants; thus, exposure to Mn poses a significant environmental health risk[1]. Further, Mn shares transporters with iron (Fe) and low levels of Fe (one of the most common nutritional deficiencies) can lead to elevated Mn uptake in the brain[2-4]. Occupational exposure to high levels of

manganese, usually via mining or smelting, can lead to a PD-like syndrome called manganism[5, 6]. Manganism has motor symptoms that closely resemble PD, likely due to the preferential accumulation of Mn in the basal ganglia, the brain region most affected in PD[6]. However, manganism can be distinguished from PD as it preferentially affects the globus pallidus instead of the substantia nigra, leading to subtly distinct motor symptoms and poor response to L-DOPA, the dopamine precursor commonly used to treat PD[6]. Despite these differences, Mn toxicity can induce many of the same pathological cascades observed in PD, such as mitochondrial dysfunction, reactive oxygen species (ROS) production, and activation of apoptotic and necrotic signaling pathways[7]. Thus, identifying pathways that contribute to Mn toxicity may enhance our mechanistic understanding of PD.

In addition to mitochondrial dysfunction and oxidative stress, impaired protein homeostasis is another prominent feature of PD[8], as well as many other age-dependent neurodegenerative diseases such as Alzheimer's disease (AD) and Huntington's disease (HD). PD patients form Lewy bodies, composed primarily of aggregated forms of the protein α-synuclein, AD patients form amyloid-β plaques and tau tangles, and HD patients form polyglutamine inclusions. Not surprisingly, many of these age-related neurodegenerative diseases show evidence of activation of the ER unfolded protein response (UPR), likely in an attempt to correct the improperly folded proteins that form these aggregates[9, 10]. Imbalances in metal homeostasis are another hallmark of age-dependent neurodegenerative diseases[11]. Elevated levels of Fe are found in affected brain regions of PD patients and pharmacological or genetic chelation of Fe has been demonstrated to halt progression of the disease in animal models of the disorder[12]. PD patients also exhibit aberrant sera levels of several metals including Mn, Fe, Cu, and Zn, further consistent with impaired metal homeostasis contributing to disease pathophysiology[13]. Several of these metals are capable of catalyzing the misfolding of aggregation/disease-prone proteins such as α-synuclein, amyloid-β, and prion proteins[11, 14, 15]. Thus, impaired metal homeostasis may help drive or exacerbate protein misfolding under disease contexts. In this study, we developed a model of manganism in the model organism *C. elegans*. We find that in addition to effects on mitochondrial function, Mn also results in activation of ER stress and impaired protein homeostasis and significantly disrupts Fe, Cu, and Ca homeostasis, key pathological features observed in many age-dependent neurodegenerative diseases.

Results

Manganese shortens lifespan and selectively disrupts iron, copper, and calcium homeostasis.
To determine if Mn affects the lifespan of *C. elegans*, we exposed worms to increasing concentrations of manganese chloride ($MnCl_2$). We found that lifetime exposure to 10 mM $MnCl_2$ had no effect on lifespan and animals appear similar to controls. At 20 mM $MnCl_2$, animals appear mostly healthy but display a significantly shortened lifespan. At 30 mM $MnCl_2$, animals appear small and decrepit and die within days, reflecting extreme toxicity (Figure 1A, Suppl. Table 1). To determine how much Mn was taken up by worms and how it might affect other metals, we performed metallomic analysis by inductively-coupled plasma (ICP) spectroscopy on young adult whole animals that had been exposed to 10 mM, 20 mM, or 30 mM $MnCl_2$ for 24 hours. As expected, we observed large increases of Mn in tissues in a dose-dependent manner (Fig. 1B). Furthermore, we observed that at 20 mM $MnCl_2$, the abundance of Fe, Ca, and strontium (Sr), a metal that behaves physiologically similar to Ca, was lower in the worms. Interestingly, at 30 mM $MnCl_2$, Fe and Cu become significantly more abundant. In contrast, we observed no significant changes in the levels of K, Mg, Na, P, S, or Zn (Fig. 1B). Based on these findings, we used 20 mM $MnCl_2$ as an intermediate dose to study Mn toxicity in future studies.

Aged animals are susceptible to manganese toxicity.
To determine how the aging process may interact with Mn toxicity, we exposed either young adult worms or worms that had been aged to day 10 of adulthood (approximately middle-aged) to 20 mM

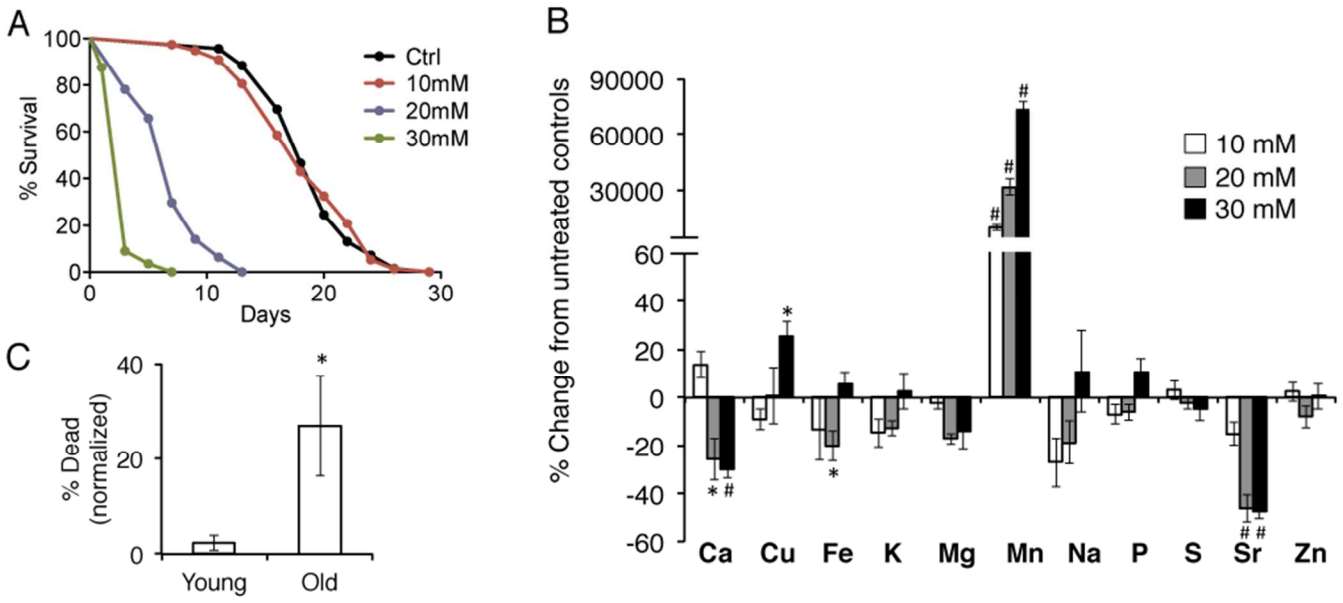

Figure 1: Manganese shortens lifespan and perturbs metal homeostasis. *A*, Lifespan of wild type N2 animals exposed to water (Ctrl), 10 mM, 20 mM, or 30mM $MnCl_2$ beginning as young adults. 20 mM and 30 mM $MnCl_2$ significantly shortens lifespan compared to controls. ($p<0.0001$, Log Rank Mantel-Cox) *B*, Metallomic ICP-AES analysis in day 1 wild type N2 young adult animals exposed to 10 mM, 20 mM, or 30 mM $MnCl_2$ for 24 hours, compared to untreated water controls. (*=$p<0.03$, #=$p<0.01$, Student's t-test compared to untreated controls) *C*, Wild type N2 day 1 or day 10 adult worms were exposed to 20 mM $MnCl_2$ and scored for lethality 48 hours later. Deaths were normalized the number of deaths in age-matched untreated controls. (*=$p<0.05$, Student's test)

$MnCl_2$ for 48-hours. Transient treatment of $MnCl_2$ had virtually no effect on the viability of young adult animals, but significantly increased mortality in aged animals (adjusted to deaths observed in untreated age-matched controls) (Fig. 1C), indicating that the aging processes sensitizes animals to Mn toxicity.

Manganese activates the mitochondrial unfolded protein response and induces mitochondrial dysfunction.

Previous studies have shown that acute exposure to manganese chloride ($MnCl_2$) can cause increased formation of ROS and mitochondrial impairment when exposed during the larval stages of *C. elegans*[16]. In this study, we examined how Mn would affect adult hermaphrodite worms. We utilized a worm strain expressing a transcriptional GFP-reporter for the mitochondrial unfolded protein response (UPR) protein, *$_p$hsp-6::GFP* [17], and exposed young adult worms to 10 mM or 20 mM $MnCl_2$ for 24 hours. Consistent with our lifespan data (Fig 1A), we found that 10 mM $MnCl_2$ was not toxic and did not elicit a mitochondrial UPR response (Fig. 2A-D). In contrast, exposure to 20 mM $MnCl_2$ elicited a robust induction of the mitochondrial UPR (Fig. 2A-D). We also found that 20 mM $MnCl_2$ severely depolarized the mitochondria in young adults as measured by tetramethylrhodamine methyl ester (TMRM) (Fig. 3), a cell-permeable fluorescent dye that is taken up by active mitochondria. Thus, our results with adult worms are consistent with previous reports that $MnCl_2$ causes mitochondrial stress and dysfunction in *C. elegans* in larval forms[16].

To test for specificity of $MnCl_2$, we exposed young adult worms to 20 mM of another divalent metal, magnesium chloride ($MgCl_2$), and found that it did not induce the mitochondrial UPR (Fig. 2E). In addition, $MnCl_2$ did not activate the transcriptional GFP-reporter for the cytoplasmic heat-shock protein, *$_p$hsp-16.2::GFP*[18], while heat stress did so as expected (Fig. 2F), indicating that $MnCl_2$ does not induce a cytoplasmic or global stress response. Thus, we observe some specificity of $MnCl_2$ to mitochondrial dysfunction in *C. elegans*.

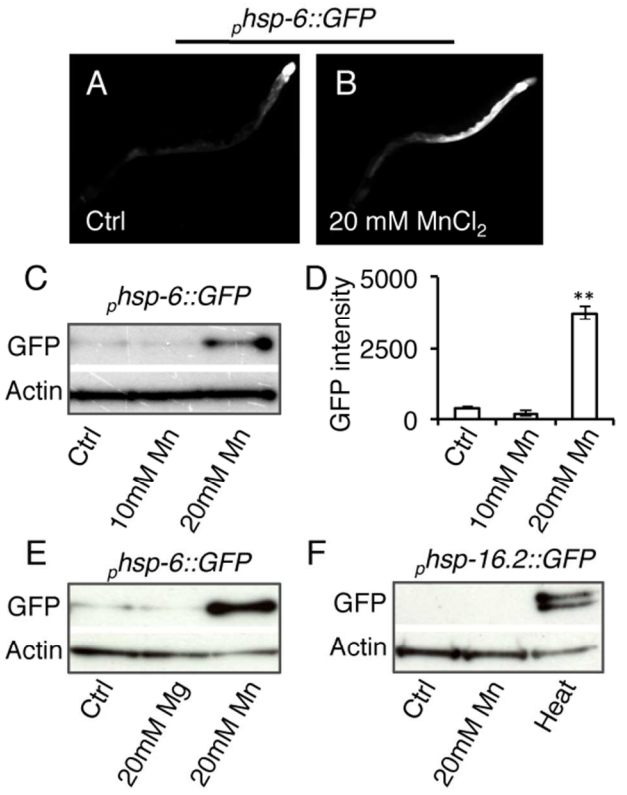

Figure 2. Acute Mn exposure activates the mitochondrial unfolded protein response. *A*, *B*, Fluorescent photomicrographs of day 1 adult hermaphrodite worms expressing *$_p$hsp-6::GFP*, a transcriptional reporter for the mitochondrial UPR, after 24 hour treatment with water (Ctrl) or 20 mM $MnCl_2$. *C*, Immunoblots of protein extracts from day 1 adult animals expressing *$_p$hsp-6::GFP* after 24 hour treatment with water (Ctrl), 10 mM, or 20 mM $MnCl_2$. *D*, Quantification of GFP intensity from *$_p$hsp-6::GFP* immunoblots in arbitrary units. (**=p<0.01, Student's t-test) *E*, Immunoblots of protein extracts from day 1 adult animals expressing *$_p$hsp-6::GFP* after 24 hour treatment with water (Ctrl), 20 mM $MgCl_2$, or 20 mM $MnCl_2$. *F*, Immunoblots of protein extracts from day 1 adult animals expressing *$_p$hsp-16.2::GFP*, a transcriptional reporter for heat stress, after 24 hour treatment with water (Ctrl), 20 mM $MnCl_2$, or a 1 hour heat stress at 33°C.

Manganese activates the ER unfolded protein response.

To determine if Mn was capable of activating UPR pathways other than the mitochondria, we next analyzed the ER UPR. We utilized the ER UPR transcriptional GFP-reporter, *$_p$hsp-4::GFP*, a homologue of the ER UPR sensing chaperone, BiP[19]. Acute exposure to 20 mM $MnCl_2$ in young adults was also found to activate the ER UPR while 20 mM $MgCl_2$ did not (Fig. 4). This suggests that in addition to effects on mitochondrial stress, Mn also elicits effects on the ER.

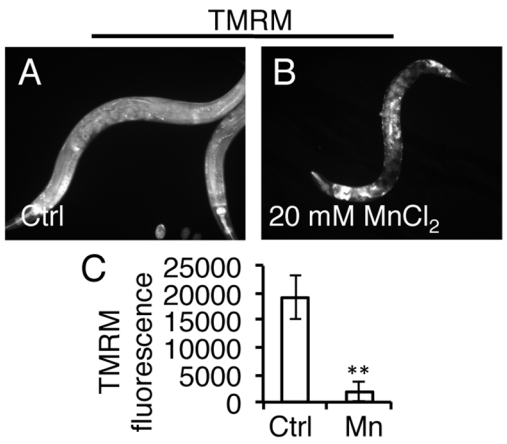

Figure 3. Acute Mn exposure depolarizes the mitochondria. *A*, *B*, Fluorescent photomicrographs of day 1 adult worms collected after 24 hour treatment with 20 mM $MnCl_2$ in the presence of TMRM. *C*, Quantification of TMRM levels in day 1 adult worms after 24 hour treatment with water (Ctrl) or 20 mM $MnCl_2$. (**=p<0.001, Student's t-test.)

Manganese antagonizes protein homeostasis in a model of protein misfolding.

To determine if elevated mitochondrial and/or ER stress correlate with dopaminergic neurodegeneration akin to that seen in human disease, we next examined the effects of acute Mn exposure in adult wild type animals whose dopaminergic neurons were labeled with GFP (*$_p$dat-1::GFP*) or in adult animals that also expressed α-synuclein in their dopaminergic neurons (*$_p$dat-1::GFP*; *$_p$dat-1::α-synuclein*) and

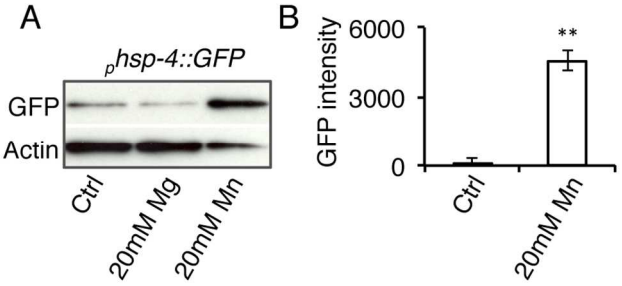

Figure 4: Acute Mn exposure activates the ER unfolded protein response. *A*, Immunoblots of protein extracts from day 1 adult animals expressing *$_p$hsp-4::GFP*, a transcriptional reporter for the ER UPR, after 24 hour treatment with water (Ctrl), 20 mM $MgCl_2$, or 20 mM $MnCl_2$. *B*, Quantification of GFP intensity from *$_p$hsp-4::GFP* immunoblots in arbitrary units. (**=p<0.001, Student's t-test)

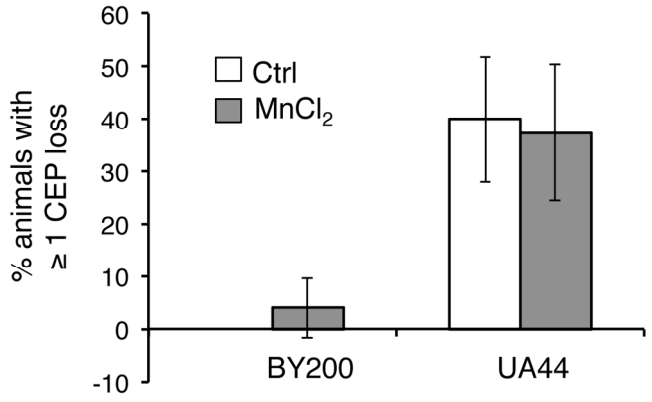

Figure 5. Mn does not cause dopaminergic degeneration in aged animals. Quantification of animals displaying dendritic loss in one or more of the their dopaminergic neurons located in the head region (CEP). Worms expressing *$_p$dat-1::GFP* (BY200) or *$_p$dat-1::GFP; $_p$dat-1::α-synuclein* (UA44) were aged until day 5 of adulthood and then exposed to water (Ctrl) or 20 mM $MnCl_2$ for 48 hours. No significant differences were observed between Ctrl and Mn-treated animals, Student's t-test.

that exhibit age-dependent neuronal degeneration[20]. We aged animals to day 5 of adulthood and then exposed aimals to 20 mM of $MnCl_2$ for 48 hours. While $MnCl_2$ was toxic as measured by organismal viability (data not shown), acute $MnCl_2$ exposure did not induce dopaminergic degeneration in control animals nor did we see additional degeneration in α-synuclein-expressing animals (Fig. 5). Conflicting reports exist as to whether $MnCl_2$ exposure results in frank dopaminergic cell loss in *C. elegans*, alone or in the context of α-synuclein expression[16, 21, 22]. Settivari et. al. and Benedetto et. al. previously reported that $MnCl_2$ causes dopaminergic degeneration in *C. elegans* when exposed as larva, whereas a more recent report by Borhorst et. al. reported that $MnCl_2$ did not induce degeneration under similar conditions[16, 21, 22]. We tested whether 50 mM $MnCl_2$ could induce dopaminergic degeneration in larval worms as originally reported[16] and observed miniscule changes in dopaminergic integrity with $MnCl_2$ treatment (100% preservation of neurons in control versus 98% preservation in $MnCl_2$ treated, data not shown), supporting the latter findings that $MnCl_2$ does not effectively induce dopaminergic degeneration.

Given that ER stress is an indication of impaired protein homeostasis, we next examined the effects of Mn in a robust model of protein misfolding. We examined a polyglutamine model in which animals express a stretch of 40 polyglutamines in their body wall muscle (AM141 [r*mIs133(P(unc-54) Q40::YFP)*])[23]. We found that exposure to 20 mM $MnCl_2$ as young adults caused

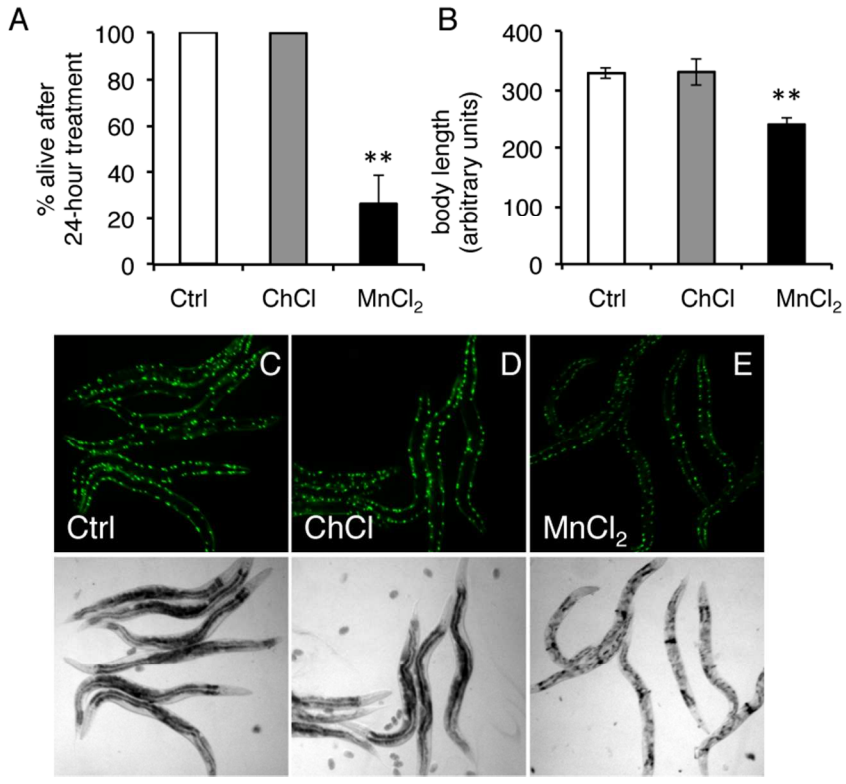

Figure 6: Acute Mn exposure is toxic in a polyglutamine model of protein misfolding. *A*, Quantification of number of day 1 animals that remained alive after a 24 hour treatment with water (Ctrl), 20 mM ChCl, or 20 mM $MnCl_2$. All animals remained alive in Ctrl and ChCl-treated animals, while only ~26% survive $MnCl_2$ treatment (**=p<0.005, Student's Test). *B*, Quantification of body length of day 1 animals after 24 hour treatment with water (Ctrl), 20 mM ChCl, or 20 mM $MnCl_2$. (**p=<0.0001, Student's t-test) *C-E*, Top panel, fluorescent photomicrographs of day 1 adults worms expressing 40 polyglutamines tagged to YFP in their body wall muscle (AM141 [*rmIs133(P(unc-54) Q40::YFP)*]) after 24 hour exposure to water (Ctrl), 20 mM ChCl, or 20 mM $MnCl_2$. Bottom panel, bright field photomicrographs from top panels.

severe toxicity that resulted in ~ 75% lethality rate after just 24 hours (Fig. 6A). Animals that remained alive were unhealthy in appearance and smaller in size (Figs. 6B-E). The effect was specific to Mn and not the chloride ion as the metabolite choline chloride ($C_5H_{14}ClNO$ abbreviated to ChCl) had no effect on polyglutamine-expressing animals at the same concentration (Fig. 6). Mn-treated animals also displayed fewer inclusions that were smaller in size (Fig. 7A,B). Further, Mn treatment altered the SDS-solubility of polyglutamine aggregates, resulting in significantly less SDS-soluble aggregates with a concomitant trend of increased SDS-insolubility, suggesting that Mn can alter protein conformation *in vivo* (Fig. 7C, D). Thus, Mn appears to significantly antagonize proteostasis in a non-neuronal model of protein misfolding.

Discussion

In this study, we describe a model of manganism in *C. elegans* that encompasses several modes of toxicity: metallomic imbalances, age-dependent susceptibility, mitochondrial and ER stress, and protein misfolding (see model, Fig. 8). Mn can directly disrupt mitochondria function and affect

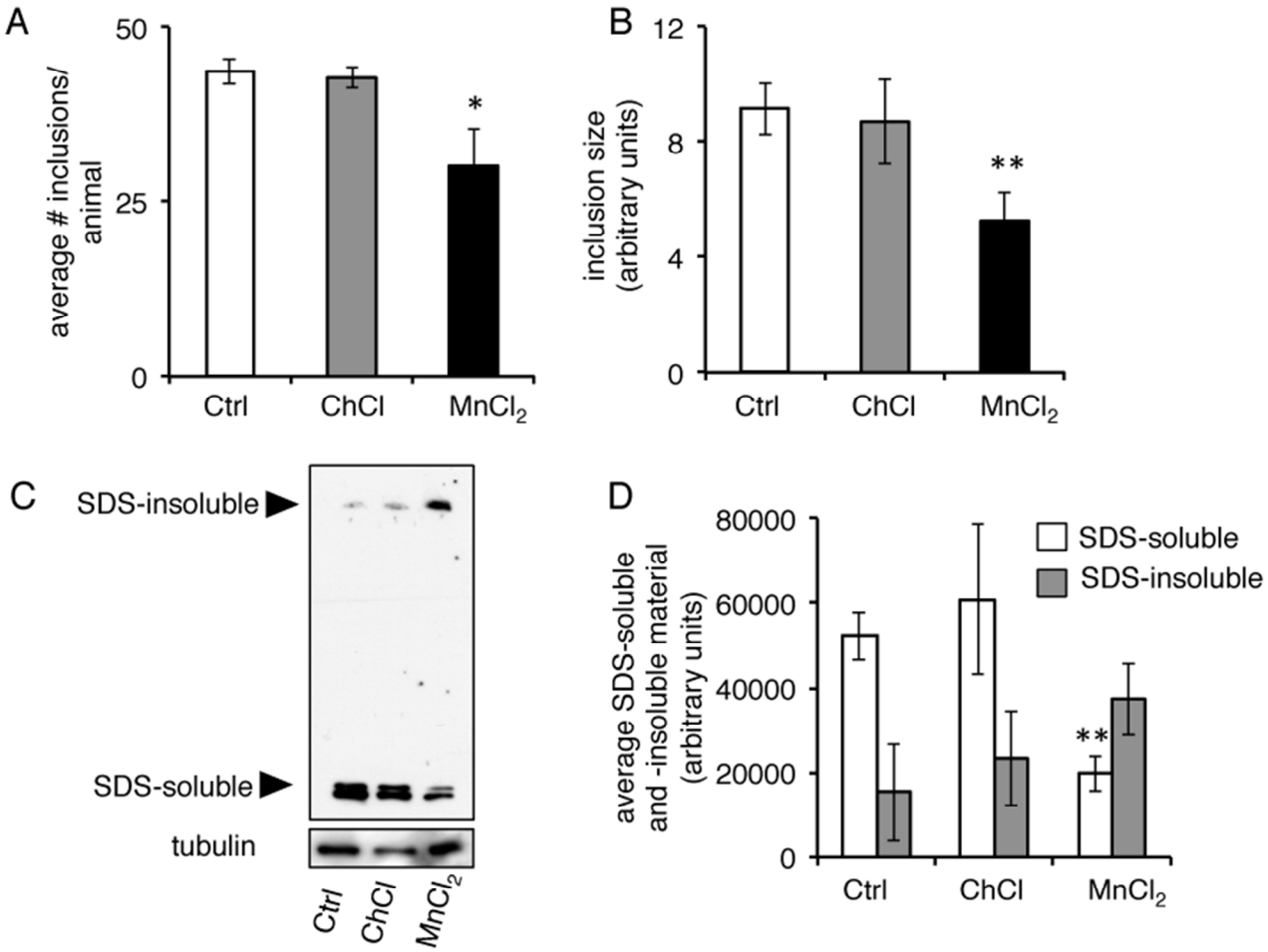

Figure 7: Acute Mn exposure alters the SDS-solubility of aggregates in a polyglutamine model. *A*, Quantification of number of YFP inclusions in day 1 adult worms expressing a 40 polyglutamine repeat tagged to YFP in their body wall muscle (AM141 [rmIs133(P(unc-54) Q40::YFP)]) after 24 hour treatment with water (Ctrl), 20 mM ChCl, or 20 mM $MnCl_2$ (*=p<0.03, Student's t-test). *B*, Quantification of relative size of YFP inclusions in day 1 animals after 24 hour treatment with water (Ctrl), 20 mM ChCl, or 20mM $MnCl_2$ (**p=<0.01, Student's t-test). *C*, Immunoblots of protein extracts from day 1 animals after 24 hour treatment with water (Ctrl), 20 mM ChCl, or 20 mM $MnCl_2$. Aggregates were separated into SDS-soluble or SDS-insoluble fractions (higher molecular weights). *D*, Quantification of SDS-soluble and -insoluble material from immunoblots (n=3, **p=<0.01, Student's t-test).

ER-mediated protein folding[7, 15]. In addition, we find that at intermediate levels of toxicity (20 mM), Mn selectively lowers Fe and Ca levels, which may further exacerbate losses in mitochondria and protein homeostasis (Fig. 8). In *C. elegans*, Mn shares transport with Fe via the divalent metal transporter (DMT-1) orthologs[2]. Thus, it is not surprising that Fe is lowered in response to excess Mn, likely as a consequence of transport competition, which has been observed in mammalian models following Mn-treatment[24, 25]. Lowered Fe in response to Mn-treatment is associated with a shift in Fe^{2+} to Fe^{3+}, which would allow Fe to more readily participate in the Fenton reaction leading to generation of free radicals and enhanced oxidative stress[24] (Fig. 8). Moreover, some evidence exists suggesting that Mn and Ca also share transporters in the mitochondria and Golgi apparatus[14, 26, 27], supporting a model in which excess Mn also outcompetes Ca for transport. In *C.elegans*, Mn and Ca appear to have similar subcellular localizations and the Golgi ATPase, PMR-1, has been identified as a Mn^{2+}/Ca^{2+} transporter[27, 28]. Lowered Ca levels are associated with impaired ER-Golgi trafficking in addition to impaired mitochondrial function[9, 29]. Crosstalk between mitochondria and ER stress may further drive pathology (Fig. 8).

Mn induces ER stress in conjunction with alterations in Ca homeostasis.

While transient activation of the ER UPR is a protective mechanism that ensures the proper folding of proteins, constitutive activation of the ER UPR is a hallmark of age-dependent neurodegenerative diseases that may further drive or exacerbate pathology[30, 31]. Previous studies have shown that Mn can upregulate the ER UPR sensor protein, BiP, in a cell model[32] and that Mn exposure in the presence of Fe deficiency can also induce ER stress and cell death[33], findings that are consistent with our results in *C. elegans*. We also observed decreased Ca levels in Mn-treated animals. Ca homeostasis has repeatedly been shown to be vital for the proper functioning of the ER. High Ca levels in the ER are important for proper function of the ER and of BiP, while depletion of Ca stores disrupts ER function and activates the ER UPR[29]. The impact of Mn on Ca homeostasis may therefore represent a novel avenue of exploration towards identifying additional mechanisms contributing to Mn toxicity.

Role of Mn in protein aggregation and aging.

Aged animals are characterized by the accumulation of insoluble proteins[34, 35], indicating that aging may be due, in part, to impaired protein homeostasis. We also observed that treatment with Mn late in life (day 10 worms) leads to a ~30% increase in mortality rate after 48 hours (normalized to untreated age-matched controls),

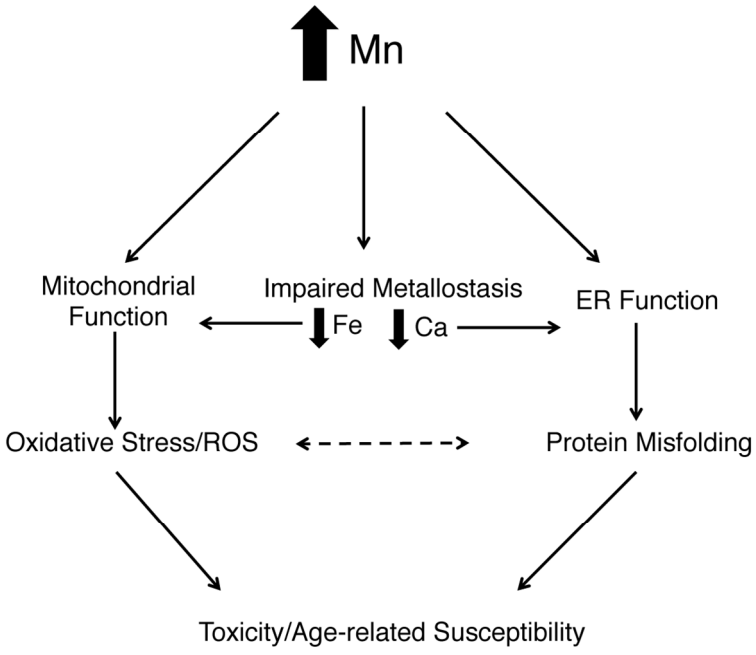

Figure 8: Modes of Mn toxicity. Schematic of potential avenues of Mn-toxicity. Mn directly affects mitochondrial function by disrupting mitochondria complex I and depleting mitochondrial ATP stores, which activates the mitochondrial stress response and stimulates ROS production, leading to toxicity and cell death. Mn can also directly perturb protein misfolding, which activates the ER stress response and leads to toxicity and cell death. Mn alters Fe homeostasis, which can lead to mitochondrial dysfunction and increase its participation in the Fenton reaction and ROS production. Mn alters Ca homeostasis, which can lead to ER dysfunction and exacerbates protein misfolding. Oxidative stress may exacerbate protein misfolding and vice versa. All pathways can eventually contribute to toxicity and cell death.

while virtually no young animals died after a 48 hour treatment. Thus, aged animals may be particularly susceptible to the mitochondrial and proteotoxic stresses of Mn due to their already impaired proteome.

Mn has been shown to stimulate the aggregation of α-synuclein *in vitro* and potentially exacerbate other neurodegenerative diseases such as amyotrophic lateral sclerosis (ALS) and prion disease[14, 15]. Here, we show that Mn also has the ability to alter aggregation states *in vivo* by shifting the unstable polyglutamine aggregates from an SDS-soluble state to a more SDS-insoluble state. Though a change in solubility of aggregates is not necessarily an indication of toxicity on its own, we concomitantly observed that Mn treatment resulted in nearly a 75% mortality rate in the polyglutamine model after just 24 hours of exposure. Animals that remained alive were decrepit and died within another 24 hours (data not shown). Thus, Mn-induced impairments in protein homeostasis combined with mitochondria dysfunction may result in widespread collapse of cellular functions and lead to rapid death in the polyglutamine model.

Mn and dopaminergic degeneration

Notably absent from our model is the ability of Mn exposure to induce dopaminergic degeneration in *C. elegans*, for which conflicting reports exist[16, 21, 22]. Previous studies have reported dopaminergic degeneration with $MnCl_2$ when exposed during larval stages. In this study, we found that $MnCl_2$ did not induce dopaminergic degeneration in either larva or aged worms, consistent with recent reports that also failed to find Mn-induced neurodegeneration[22]. Authors from this study cited the purity of the $MnCl_2$ batches used as a possible discrepancy between their results and those reported previously. Taken together, our results suggest that $MnCl_2$ does not directly target dopaminergic neurons. Close analysis of patient cases of manganism show that the region of the basal ganglia most affected by Mn is the globus pallidus, which receives inputs downstream of the dopaminergic-rich substania nigra[6]. Thus, Mn may only indirectly affect dopaminergic outputs rather than having direct affects on dopaminergic neurons.

Conclusions

Given the multifactorial causes of PD, *C. elegans* provides a tractable model to study the combined impact of environment, age, and genetic susceptibilities. Our findings suggest the modeling manganism in *C. elegans* could provide a platform for drug discovery that could lead to the identification of therapeutic avenues that allow a better understand of these factors as they relate to the interplay between mitochondrial dysfunction, protein misfolding, and metallomic imbalances.

Methods

C. elegans strains

The following strains were cultured using standard conditions and can be obtained via the *Caenorhabditis* Genetics Center (CGC, University of Minnesota)[36]: N2 Bristol (wild type), SJ4100 [*zcIs13(hsp-6p::GFP)*], SJ6 [*zcIs4(hsp-4p::GFP)*], CL2070 [*dvIs70(phsp16.2p::GFP; rol-6(su1006)*], and BA671 [*spe-9(hc88)*]. The following were kind gifts from the following laboratories: BY200 [*vtIs1(pdat-1::GFP)*] (provided by Aschner laboratory, Vanderbilt University)[22], UA44 [*baIn11(pdat-1::α-synuclein, pdat-1::GFP)*] (provided by Caldwell laboratory, University of Alabama)[20], and AM141 [*rmIs133(P(unc-54) Q40::YFP)*] (provided by Morimoto laboratory, Northwestern University)[23].

Preparation on manganese plates

Stock solutions of 3M manganese (II) chloride tetra-hydrate (Sigma-Aldrich) were made in deionized/distilled water immediately before use. $MnCl_2$ solution was added directly to NGM plates at the indicated final concentrations. *E. coli* OP50 was spotted on NGM plates and spread by gently swirling and allowed to grow for 24 hours at room temperature. Plates were stored at 4°C for no longer than 2 weeks.

Microscopy and quantification

Day 1 adult worms were collected and paralyzed in 1mM levamisole, mounted on agar pads with glass coverslips, and analyzed using an Olympus BX51

upright microscope. Worms expressing GFP were analyzed using 470/40 nm excitation and 525/50 nm emission wavelengths. Worms exposed to TMRM were analyzed using 535/50 nm excitation and 610/75 nm emission wavelengths. Approximately 20 animals per condition were used and fluorescent intensity was normalized to the body-length (mid-line length of the animal). Quantification of pixel densities and polyglutamine inclusions were analyzed with Image J™. All experiments were repeated at least three times with similar results.

Western blot assays
For western blots, approximately 20-40 worms were collected at day 1 of adulthood. Worms were flash frozen and resuspended in a final concentration of 2% SDS sample buffer with 2.5% β-mercaptoethanol. Immunoblots were probed with anti-mouse GFP (B2) (Santa Cruz Biotechnology, 1:1000) or anti-rabbit tubulin (LL-17) (Sigma Aldrich, 1:1000) for loading controls.

TMRM assays
To assess mitochondrial membrane potential, N2 wild type worms were reared from synchronized eggs at 20°C until the 4th larval stage and then transferred to control plates or plates containing $MnCl_2$ in the presence of tetramethylrhodamine methyl ester (TMRM). TMRM was prepared as previously described to a final concentration of 0.1uM in NGM agar plates[17]. Worms were collected for microscopic analysis and quantified 24 hours later.

Scoring of dopaminergic degeneration
Synchronous populations of worms were aged until day 5 of adulthood at 20°C and then transferred to control or $MnCl_2$ plates. After 48 hours, animals were collected for microscopic analysis. Animals were scored as having 0, 1, 2, 3, or 4 cephalic dendrites as measured by GFP fluorescence. Approximately 30 animals per condition were used and experiments were repeated at least three times with similar results.

Polyglutamine analysis
AM141 [*rmIs133(P(unc-54) Q40::YFP)*] worms were grown at 20°C until the 4th larval stage and then transferred to control or $MnCl_2$ plates and simultaneously shifted to 25°C. After 24 hours, worms were collected for analysis for western blot, for microscopy, or for survival (scored by gentle prodding).

Lifespan analysis
Synchronized populations of worms were cultured at 20°C and transferred to control or $MnCl_2$ plates beginning as young adults that had been supplemented with 10μg/μl 5-fluoro 2-deoxyuridine (FUdR) to prevent progeny production. Animals that crawled off the plates or died due to internal gut or vulval extrusions were censored from the population. We found that in the absence of FUdR, concentrations higher than 10 mM $MnCl_2$ elicited high levels of matricide (larval explosions), thus making lifespan analysis difficult to interpret (data not shown). Log rank (Mantel-Cox) statistics were used for analysis of lifespans using Prism™.

Inductively-coupled plasma atomic emission spectroscopy analysis
ICP analysis was conducted as previously described[37]. Briefly, synchronized populations of arrested L1s were grown en masse (25,000-40,000 worms) at 25°C to induce sterility in the temperature-sensitive mutant, *spe-9(hc88)*. Worms were shifted to control or $MnCl_2$ plates at the 4th larval stage worms and collected in M9 buffer 24 hours later. Worms were washed three times in M9 buffer and a final wash in 150 mM choline chloride, 1mM HEPES. Worms were dried at 60°C for 48 hours. Dried pellets were acid digested with Omnitrace 70% HNO_3 at 60°C overnight. Samples were diluted with Omnitrace water for a final concentration of 5% HNO_3.

Acknowledgements

We thank members of the Lithgow and Andersen laboratories for helpful discussion. We thank Tai C. Holland for technical support for ICP analysis. This work was supported by a Larry L. Hillblom Foundation grant as well as NIH grants (R21 AGGSS2620). S.A. was supported by NIH

Training Grants AG000266 and 1F32ES022370-01A1.

Notes

[a] Buck Institute For Research on Aging, 8001 Redwood Blvd. Novato, CA 94945 USA
[b] Nutrition & Metabolism Center, Children's Hospital Oakland Research Institute, Oakland, CA, USA

References

1. M. Aschner, K. M. Erikson, E. Herrero Hernandez and R. Tjalkens, *Neuromolecular medicine*, 2009, 11, 252-266.
2. C. Au, A. Benedetto, J. Anderson, A. Labrousse, K. Erikson, J. J. Ewbank and M. Aschner, *PloS one*, 2009, 4, e7792.
3. K. M. Erikson, Z. K. Shihabi, J. L. Aschner and M. Aschner, *Biological trace element research*, 2002, 87, 143-156.
4. C. Au, A. Benedetto and M. Aschner, *Neurotoxicology*, 2008, 29, 569-576.
5. B. A. Racette, *Neurotoxicology*, 2013.
6. C. W. Olanow, *Annals of the New York Academy of Sciences*, 2004, 1012, 209-223.
7. A. Benedetto, C. Au and M. Aschner, *Chemical reviews*, 2009, 109, 4862-4884.
8. D. J. Moore, A. B. West, V. L. Dawson and T. M. Dawson, *Annu Rev Neurosci*, 2005, 28, 57-87.
9. T. Cali, D. Ottolini and M. Brini, *BioFactors (Oxford, England)*, 2011, 37, 228-240.
10. D. Lindholm, H. Wootz and L. Korhonen, *Cell Death Differ*, 2006, 13, 385-392.
11. K. J. Barnham and A. I. Bush, *Current opinion in chemical biology*, 2008, 12, 222-228.
12. D. Kaur, F. Yantiri, S. Rajagopalan, J. Kumar, J. Q. Mo, R. Boonplueang, V. Viswanath, R. Jacobs, L. Yang, M. F. Beal, D. DiMonte, I. Volitaskis, L. Ellerby, R. A. Cherny, A. I. Bush and J. K. Andersen, *Neuron*, 2003, 37, 899-909.
13. S. S. Ahmed and W. Santosh, *PloS one*, 2010, 5, e11252.
14. A. B. Bowman, G. F. Kwakye, E. Herrero Hernandez and M. Aschner, *J Trace Elem Med Biol*, 2011, 25, 191-203.
15. A. Santner and V. N. Uversky, *Metallomics : integrated biometal science*, 2010, 2, 378-392.
16. R. Settivari, J. Levora and R. Nass, *The Journal of biological chemistry*, 2009, 284, 35758-35768.
17. T. Yoneda, C. Benedetti, F. Urano, S. G. Clark, H. P. Harding and D. Ron, *Journal of cell science*, 2004, 117, 4055-4066.
18. C. D. Link, J. R. Cypser, C. J. Johnson and T. E. Johnson, *Cell stress & chaperones*, 1999, 4, 235-242.
19. M. Calfon, H. Zeng, F. Urano, J. H. Till, S. R. Hubbard, H. P. Harding, S. G. Clark and D. Ron, *Nature*, 2002, 415, 92-96.
20. Q. Ruan, A. J. Harrington, K. A. Caldwell, G. A. Caldwell and D. G. Standaert, *Neurobiology of disease*, 2010, 37, 330-338.
21. A. Benedetto, C. Au, D. S. Avila, D. Milatovic and M. Aschner, *PLoS genetics*, 2010, 6.
22. J. Bornhorst, S. Chakraborty, S. Meyer, H. Lohren, S. Grosse Brinkhaus, A. L. Knight, K. A. Caldwell, G. A. Caldwell, U. Karst, T. Schwerdtle, A. Bowman and M. Aschner, *Metallomics : integrated biometal science*, 2014, 6, 476-490.
23. J. F. Morley, H. R. Brignull, J. J. Weyers and R. I. Morimoto, *Proceedings of the National Academy of Sciences of the United States of America*, 2002, 99, 10417-10422.
24. K. Fernsebner, J. Zorn, B. Kanawati, A. Walker and B. Michalke, *Metallomics : integrated biometal science*, 2014, 6, 921-931.
25. N. Moldovan, A. Al-Ebraheem, N. A. Miksys, M. J. Farquharson and N. A. Bock, *Biometals*, 2013, 26, 179-187.
26. C. E. Gavin, K. K. Gunter and T. E. Gunter, *Neurotoxicology*, 1999, 20, 445-453.
27. K. Van Baelen, J. Vanoevelen, L. Missiaen, L. Raeymaekers and F. Wuytack, *The Journal of biological chemistry*, 2001, 276, 10683-10691.
28. G. McColl, S. A. James, S. Mayo, D. L. Howard, C. G. Ryan, R. Kirkham, G. F. Moorhead, D. Paterson, M. D. de Jonge and A. I. Bush, *PloS one*, 2012, 7, e32685.
29. M. A. Brostrom and C. O. Brostrom, *Cell Calcium*, 2003, 34, 345-363.
30. J. A. Moreno, H. Radford, D. Peretti, J. R. Steinert, N. Verity, M. G. Martin, M. Halliday, J. Morgan, D. Dinsdale, C. A. Ortori, D. A. Barrett, P. Tsaytler, A. Bertolotti, A. E. Willis, M. Bushell and G. R. Mallucci, *Nature*, 2012, 485, 507-511.
31. M. Halliday and G. R. Mallucci, *Neuropharmacology*, 2014, 76 Pt A, 169-174.
32. H. S. Chun, H. Lee and J. H. Son, *Neuroscience letters*, 2001, 316, 5-8.
33. Y. A. Seo, Y. Li and M. Wessling-Resnick, *Neurotoxicology*, 2013, 38, 67-73.
34. D. C. David, N. Ollikainen, J. C. Trinidad, M. P. Cary, A. L. Burlingame and C. Kenyon, *PLoS biology*, 2010, 8, e1000450.
35. P. Reis-Rodrigues, G. Czerwieniec, T. W. Peters, U. S. Evani, S. Alavez, E. A. Gaman, M. Vantipalli, S. D. Mooney, B. W. Gibson, G. J. Lithgow and R. E. Hughes, *Aging cell*, 2011.
36. H. J. Sulston J, in *The Nematode Caenorhabditis elegans*, ed. W. B. W., Cold Spring Harbor Laboratory Press Cold Spring Harbor, 1988, pp. 587-606.
37. K. E. Page, K. N. White, C. R. McCrohan, D. W. Killilea and G. J. Lithgow, *Metallomics : integrated biometal science*, 2012, 4, 512-522.

